International Journal of Power Electronics and Drive Systems (IJPEDS)
Vol. 13, No. 2, June 2022, pp. 1129~1139
ISSN: 2088-8694, DOI: 10.11591/ijpeds.v13.i2.pp1129-1139

An algorithm to extract the maximum power from the PV-based generation systems under non-uniform weather

Issam A. Smadi, Ahmad AL-Ramaden
Electrical Engineering Department, Jordan University of Science and Technology, Irbid, Jordan

Article Info

Article history:

Received Sep 18, 2021
Revised Mar 21, 2022
Accepted Apr 1, 2022

Keywords:

Hidden points
LabVIEW
Maximum power
Non-uniform conditions
PV generation system

ABSTRACT

This paper presents a fast and simple algorithm to extract the maximum power under non-uniform weather from the photovoltaic (PV) based generation systems. The proposed algorithm's three stages are the scanning stage, the tracking stage, the detecting and avoiding the hidden points stage. The hidden points are caused by a transition between the global maximum power point (GMPP) and a local maximum power point (LMPP) when the partial shading conditions (PSCs) are changed. This transition cannot be observed by monitoring only the power difference of the PV generation system. Simulation results with comparisons to other algorithms developed for global maximum power point tracking (GMPPT) under PSCs are provided to clarify and show the effectiveness of the proposed GMPPT algorithm. The average tracking speed of the proposed algorithm is two times faster than the compared MPPT algorithms, with about 2% more power generated with no additional cost. Moreover, the proposed GMPPT algorithm is implemented in real-time using National Instruments (NI) CompactRIO in field-programmable gate array (FPGA) mode to confirm the applicability of the proposed work.

Corresponding Author:

Issam A. Smadi
Electrical Engineering Department, Jordan University of Science and Technology
3030, Ar-Ramtha, Irbid, Jordan
Email: iasmadi@just.edu.jo

1. INTRODUCTION

Photovoltaic (PV) based power generation systems are among the key players in the world's future energy mix due to their cost-effectiveness and the advanced ability to connect them to the grid [1]. However, some issues still need to be addressed to maximize the output energy from the PV-based power generation systems. One of the emerging issues is the extraction of the maximum power under non-uniform weather [2]–[4]. The hill-climbing and its related maximum power point tracking (MPPT) algorithms, such as perturb and observe (P&O) [5]–[7] and incremental conductance (INC) [8]–[10] are simple and powerful methods in locating the maximum power point under uniform conditions. However, under non-uniform weather, they may be stuck at a local maximum power point (LMPP) because of the existence of multiple maxima in the power-voltage (P–V) curve [11].

PV based power generation systems with reconfigurable PV modules were investigated in [12] and [13] to minimize energy drop due to the partial shading effect. Although reconfiguration techniques can produce higher output power than the fixed configuration in the PV based power generation systems, reconfiguring the PV modules' location is not trivial and needs additional hardware. This will cause higher costs and greater system complexity.

The artificial bee colony (ABC) is adopted to detect the partial shading conditions (PSCs) and the P&O is used to locate the global maximum power point (GMPP) in [14], forming a two-stage MPPT algorithm. Another two-stage global maximum power point tracking (GMPPT) algorithm is proposed in [15], where particle swarm optimization (PSO) is responsible for detecting the PSC and the P&O is accountable for the final GMPP tracking. Statistical evaluations of different MPPT algorithms based on stochastic optimization techniques regarding stability, success rate, and convergence speed are done in [16] and [17]. However, as in any stochastic optimization technique locating the global maxima is not guaranteed, which may cause energy loss. Besides, the time to track the GMPP in these techniques is relatively long.

Other GMPPT algorithms divide the P–V curve into several voltage segments. Then at each voltage segment, the LMPP is tracked using P&O or related MPPT methods. The GMPP is then located comparing all LMPPs [18]–[20]. The module open-circuit voltage (V_{oc}^{MOD}) of the PV array is usually used for voltage segmentation where $0.8\,V_{oc}^{MOD}$ is adopted in [18] while $0.5\,V_{oc}^{MOD}$ is preferable in [19]. How much fraction from the V_{oc}^{MOD} suffices to track the GMPP is unclear, and the actual GMPP can be missed if the voltage step is not adequately selected [20]. Also, the transient voltage of the PV generation system must be wisely taken care of while scanning the P–V curve; otherwise, misleading LMPPs will be registered instead of the actual LMPPs.

Ghasemi *et al*. [21] replaced the voltage step scanning with ramp function scanning to mitigate the PV voltage transient effect on the MPP. The work in [22] uses the current variation to detect the MPP at sampling multiple of V_{oc}^{MOD}, then the hill-climbing algorithm is called when a peak is detected to locate the exact LMPP. By estimating an upper power limit for each sub-region at some samples of the I-V curve, the search region is minimized in [23]. The procedure will continue until the voltage segment length is less than the V_{oc}^{MOD}, then the GMPPT is located using P&O. This method may fail if the peak points are closed to each other.

The algorithms above cannot deal with the hidden points because they rely on power variation to detect partial shading (PS). The hidden points are points in the P–V curve caused by a transition between the GMPP and LMPP when the PSCs are changed, which cannot be observed by monitoring only the power difference of the PV-based power generation system. Therefore, this paper proposes an effective and fast algorithm to extract the maximum power from the PV based power generation systems under non-uniform conditions by detecting the quasi-maximum points based on the current variation that can detect the hidden point. Besides the forward scanning, the proposed algorithm also tracks the GMPP using reverse scanning with termination criterion, reducing the search space dramatically. Comparisons with other algorithms developed for MPPT under PSCs are considered clarifying and showing the effectiveness of the proposed method. Finally, the proposed MPPT algorithm is implemented in real-time using national instruments (NI) CompactRIO in field-programmable gate array (FPGA) mode to demonstrate the viability of the proposed work.

This paper is organized as: the effect of PSC on the PV-based power generation systems is revisited, and the definition of the hidden point is given in section 2. Section 3 introduces the proposed GMPPT algorithm. Numerical comparisons with other algorithms developed for MPPT under PSCs are provided in section 4. Experimental validation is discussed in section 5. Finally, conclusions are given in section 6.

2. PV BASED POWER GENERATION SYSTEMS

2.1. PV based power generation system characteristic under partial shading

Several PV modulus configurations are adopted in practice to achieve the desired PV based power generation sizing. Without loss of generality, the PV generation system shown in Figure 1 is taken as an example to highlight the partial shading effect and define the hidden points. Because of different obstacles like shadows, moving clouds, and snow, the solar panels in the PV array are not facing the same weather. The non-uniform weather causes partial shading effects in the PV modules. The current produced by the shaded PV module is less than the other shine modules. This may damage the shaded module or reduce the generated power from the PV array. A bypass diode is connected to each module to protect the shaded module and minimize the power losses, as shown in Figure 1. The bypass diodes short-circuit the shaded modules to prevent them from operating at negative voltage [24]. However, multiple peaks exist in the P-V curve because of the activation of the bypass diodes Figure 2, assuming two different weather. The existence of multiple peaks puts stress on the adopted MPPT algorithm and may lead to tracking failure.

2.2. The effect of the hidden points on MPPT

Most of the GMPPT algorithms proposed in the literature use a power variation threshold (i.e., $|\Delta P| \geq 5\%$) to detect the weather change [25]. However, monitoring the power variation alone, it is difficult to notice the change in weather. Figure 3 shows a PV generation system under different weathers, in which

Figure 3(a) shows the PV generation system under uniform weather, while Figures 3(b) and 3(c) under non-uniform weather. Figure 3(d) shows the P-V curves under uniform and non-uniform weather. Let the GMPP be located when the PV generation system faces the first partial shading condition (PSC_1). The weather changed after some time and the PV generation system met another partial shading condition (PSC_2). While the irradiance shifts between PSC_1 and PSC_2, the old GMPP was preserved as a new LMPP with no power variation. Hence, any GMPPT algorithm relying on power variation cannot figure out this transition in weather. In this paper, this point is called the partial shading hidden point (PSHP). The existence of the PSHP reduces the maximum generated power; hence, it must be avoided. The proposed GMPPT algorithms can figure out the presence of PSHPs and avoid them without additional cost or burden.

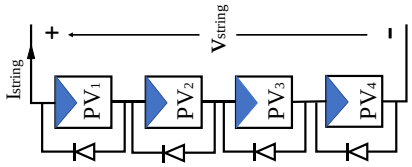

Figure 1. PV based power generation system

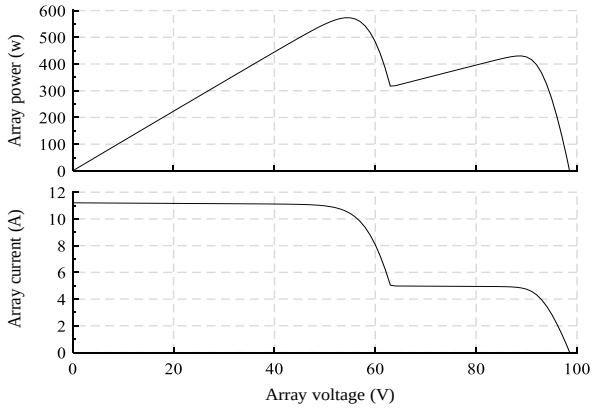

Figure 2. The P–V and I–V curves for a shaded PV array under non-uniform weather

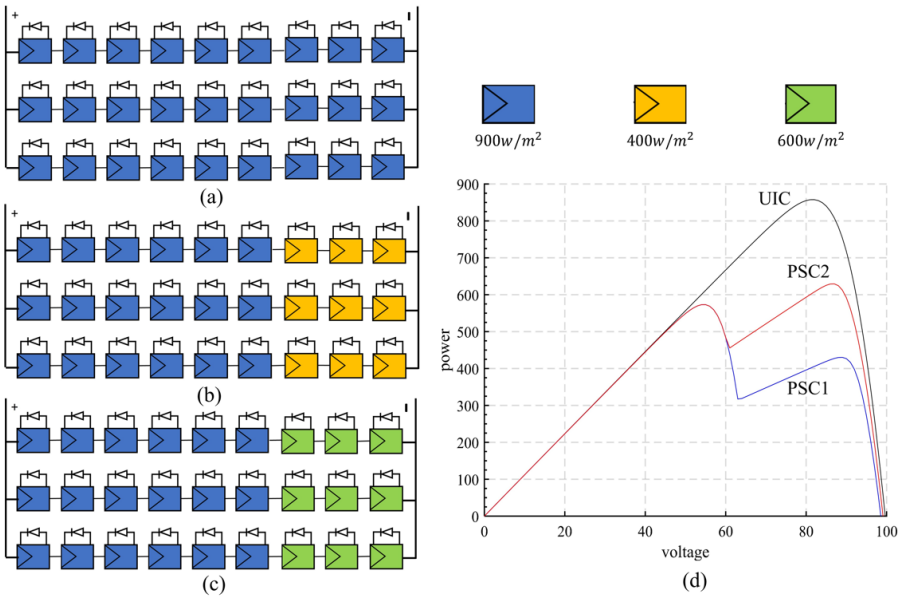

Figure 3. Series-parallel configurations PV generation system under different weathe (a) uniform irradiance condition (UIC), (b) partial shading condition 1 (PCS1), (c) partial shading condition 2 (PCS2), and (d) P-V curves under different weather

3. THE PROPOSED GMPPT METHOD

Three simple stages form the proposed algorithm: the scanning stage in which all the quasi-maximum power points are located and stored. The maximum of these points is passed to the second stage to find the exact GMPPT employing P&O. A hidden point stage is adopted to bypass the PSHP in the P–V curve if it exists. Moreover, the reverse scanning procedure is integrated with the proposed work to minimize the search space. Figure 4 shows the flowchart of the proposed GMPPT algorithm, and the detailed description of each stage is discussed in the following sections.

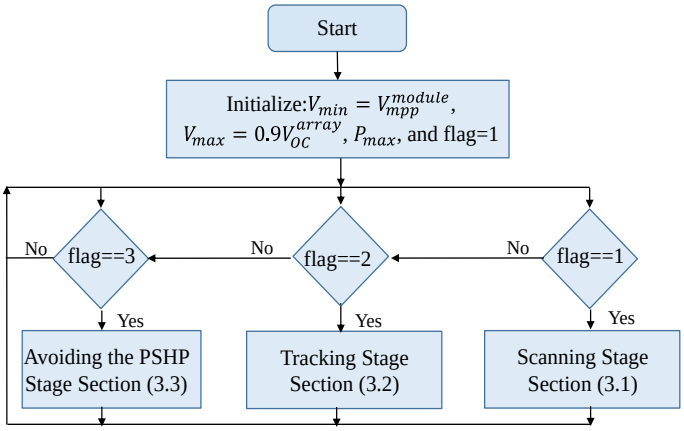

Figure 4. The flowchart of the proposed MPPT algorithm

3.1. Scanning the P–V curve stage

3.1.1. Forward scanning

Scanning the PV curve can be either forward or reverse Figure 5. In forwarding direction scanning (Figure 5(a)), the reference voltage is updated from a lower voltage (V_{min}) to an upper voltage (V_{max}).

$$V_{ref}(kT_s) = V_{ref}\big((k-1)T_s\big) + \Delta V \quad (1)$$

where k is an integer number, T_s is the sampling time, kT_s is the current sample, $(k-1)T_s$ is the previous sample, and ΔV is the voltage step. The DC-DC converter duty cycle is regulated to follow the reference voltage of the PV generation system. At each sample, the current is sensed, and the current variation is calculated using:

$$\Delta I = \left|\frac{I(KT_s) - I\big((K-1)T_s\big)}{I\big((K-1)T_s\big)}\right| \quad (2)$$

The first instant at which $\Delta I \geq 5\%$ is detected is the nearest to the actual peak, as shown in Figure 6. Therefore, an MPP is detected; this point is saved as a quasi-local maximum power point (QLMPP). The switch in the flowchart of Figure 5(a) is adopted for this purpose. According to Figure 5, updating the voltage reference is ended if the saved QLMPPs is equal to the number of series modules or the reference voltage hits the maximum limit. Normally, $V_{min} = V_{mpp}^{module}$ and $V_{max} = 0.9V_{OC}^{array}$ [23].

3.1.2. Reverse scanning

In the reverse scanning (Figure 5(b)), the current at V_{min} is sensed and registered as I_{max}. Then, the P–V curve scanning is done from V_{max} toward V_{min} updating V_{ref} as in (3) while monitoring the PV current as in (2).

$$V_{ref}(kT_s) = V_{ref}\big((k-1)T_s\big) - \Delta V \quad (3)$$

In the reverse scanning, the last occurrence of $|\Delta I| \geq 5\%$ is the closest to the actual peak, as demonstrated in Figure 6. Therefore, at this point, an MPP is detected and saved as a QLMPP. The switch in the flowchart of Figure 5(b) is adopted for this purpose. The scanning is ended if either the PV current holds $I_{pv} \geq 0.95I_{max}$ or the minimum voltage is reached.

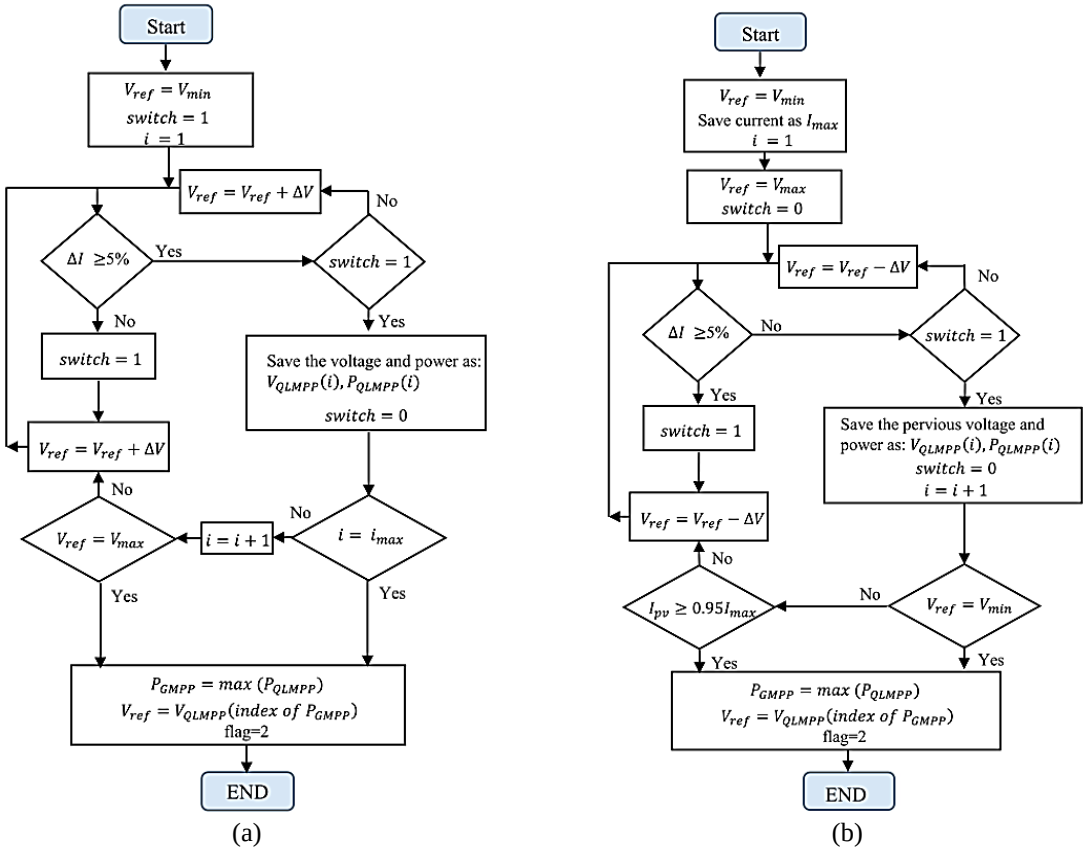

Figure 5. Scanning the P–V curve stage adopting (a) forward scanning (b) reverse scanning

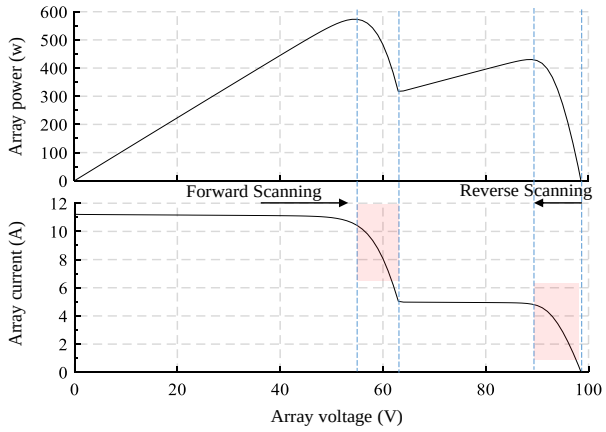

Figure 6. P–V curve forward and reverse scanning

3.2. GMPPT and partial shading detection

In this stage, the P&O will take the maximum of the stored QLMPP to track the actual GMPP (Figure 7(a)). During this stage, the power variation is found using:

$$\Delta P = \left| \frac{P(kT_S) - P\left((k-1)T_S\right)}{P\left((k-1)T_S\right)} \right| \quad (3)$$

If ΔP ≥ 5%, then the weather changes, and the algorithm will activate stage 3.1, scanning the P–V curve. If there is no variation in power for a threshold time, the algorithm will call stage 3.3, avoiding hidden points (Figure 7(b)).

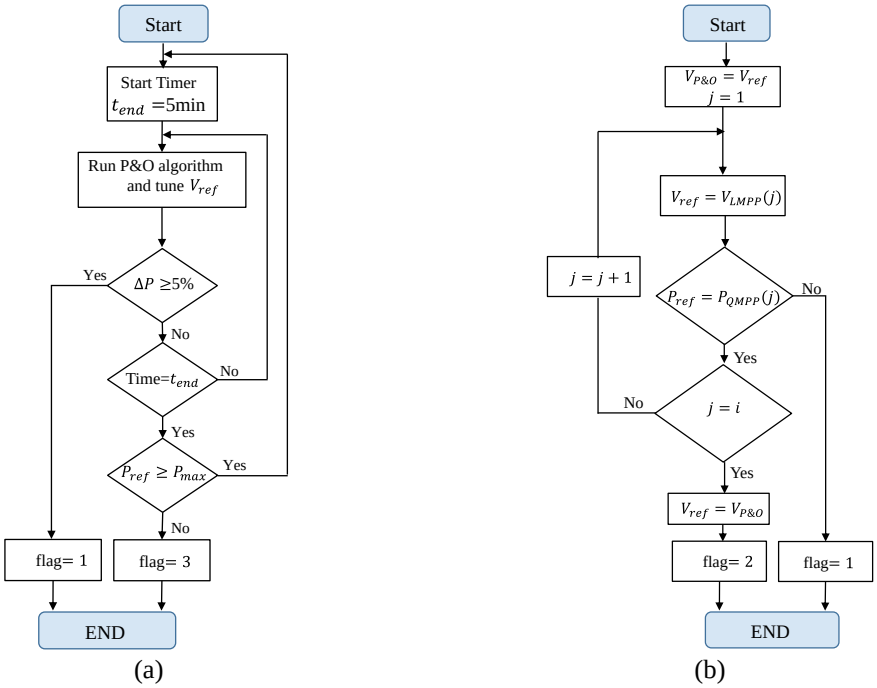

Figure 7. GMPPT and PS detection (a) tracking stage (b) avoiding the hidden point stage

3.3. Avoiding hidden point

To prevent the PSHP, a timer is activated once the P&O tracks the actual GMPP. If a threshold time is over without detecting PSC observing the variation in power, the algorithm will check the saved QLMPPs, as shown in the flow chart of Figure 7(b). If there is any variation in the stored QLMPP power, the algorithm will detect a PSC and activate stage 3.1. If no change in power is noticed, the timer is initialized, and the algorithm will call stage 3.2, tracking and monitoring the power variation (Figure 7(a)).

4. NUMERICAL SIMULATION

The proposed GMPPT method in this work is independent of the adopted PV generation system configuration. Thus, the series-parallel configuration shown in Figure 3 is nominated without loss of generality. The simulated sub-modules and system parameters are given in Table 1. Figure 8 shows the implementation of the proposed GMPPT algorithm in which a buck-boost DC-DC converter interfaces the PV generation system to a load.

Table 1. The sub-module and simulation parameters

Parameters	Symbole	Value
Output power	P_{max}	35 W
Open circuit voltage	V_{OC}^{mod}	11.1 V
Short circuit current	I_{sc}^{mod}	4.15 A
Voltage at P_{max}	V_{mpp}^{mod}	9V
Current at P_{max}	I_{mpp}^{mod}	3.89 A
Buck-Boost inductance	L	1 mH
Input side capacitance	C_{in}	470 µF
Output side capacitance	C_{out}	100 µF
Switching Frequency	f_s	20 kHz
Resistive load	R_L	100

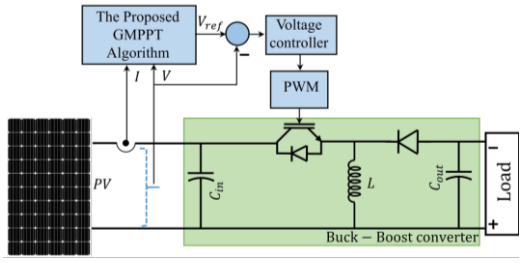

Figure 8. The implementation of the proposed GMPPT algorithm

4.1. Hidden point simulation

This simulation verifies the capability of the proposed GMPPT algorithm to detect and avoid the PSHP. The forward scanning-based algorithm (Figure 5(a)) is nominated without loss of generality. The simulation will mimic the scenarios shown in Figure 3 and uses the system shown in Figure 8. Three kinds of weather are taking place: a UIC for one second, PSC1 for another one second, and PSC_2 for the remaining

time of the simulation. The proposed algorithm starts with the scanning stage and finds one peak (P = 850 W) at (V = 80 V). The P&O finds the actual GMPP (P = 853.3 W) at (V = 81.7 V) while monitoring the power. The hidden point stage of the proposed method is activated once the timer hits the timer threshold.

Under UIC, no change in power has been detected; hence, the algorithm returns to stage 3.2. A PSC is detected at 0.9 sec.; hence the algorithm initiates stage 3.1, locating two QLMPP. The maximum among them is passed to stage 3.2, and the P&O finds the GMPP. At 1.4 sec., the threshold time is reached, and stage 3.3 is activated. The algorithm examines the saved QLMPP; no power variation is noticed, indicating no weather change. Therefore, the timer is initialized, and stage 3.2 is triggered. A change in the weather occurs at t =1.9 sec., with an LMPP equal to the previous GMPP. Hence, any algorithm that relies on the power variation will fail. However, the proposed algorithm can detect this event by checking the saved QLMPPs power. A change in power is noticed. Thus, stage 3.1 is called. Figure 9 shows the results that clarify and demonstrate the proposed method's capability to overcome the PSHPs.

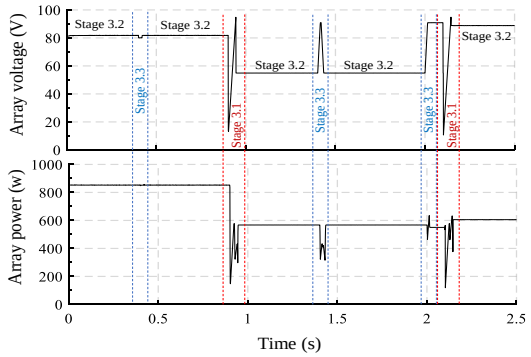

Figure 9. The hidden point simulations

4.2. Comparisons with other methods

Comparisons with the works given in [22], [23] are carried out to demonstrate the effectiveness of the proposed GMPPT algorithm. Figure 10 shows the P–V curve under different weather conditions. At first, the UIC1 occurs between $t\epsilon[0,0.59)$ sec. At t=0.59 sec, PSC1 occurs until t=1.47 sec, followed by PSC_2 until 2.2 sec, and UIC2 until t=3.5 sec. Adopting the forward scanning, all the voltage range between V_{min} and V_{max} is scanned, while it is unnecessary to examine all the voltage range in the reverse scanning method. Figure 11 shows the browsed voltage range adopting the reverse scanning under each condition. Figure 12 shows the comparison between the proposed and other algorithms, in which Figure 12(a) depicts the results of the proposed method adopting the forward scanning. In contrast, Figure 12(b) shows the results of the proposed method assuming reverse scanning. Figures 12(c) and 12(d) show the results adopting the approximate I-V and the PV current variation-based methods, respectively. Figure 13 shows a zoom-in of comparing the proposed and other algorithms. Figures 12 and 13 show that although all utilized methods can track the GMPP, the proposed method has the shortest tracking time. Hence, the higher average power is generated adopting the proposed method. A summary of the results is given in Table 2.

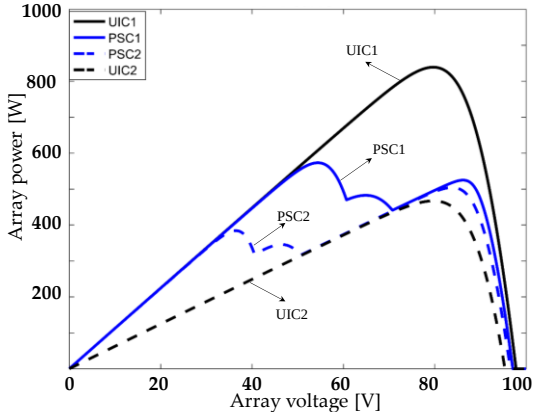

Figure 10. P–V curves under different PSC

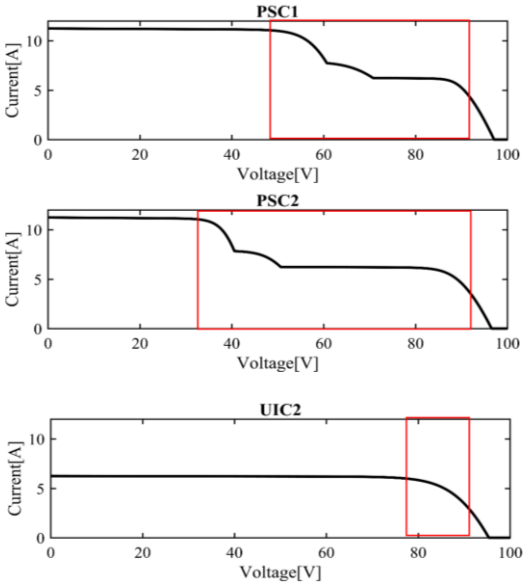

Figure 11. The browsed voltage range adopting the reverse scanning

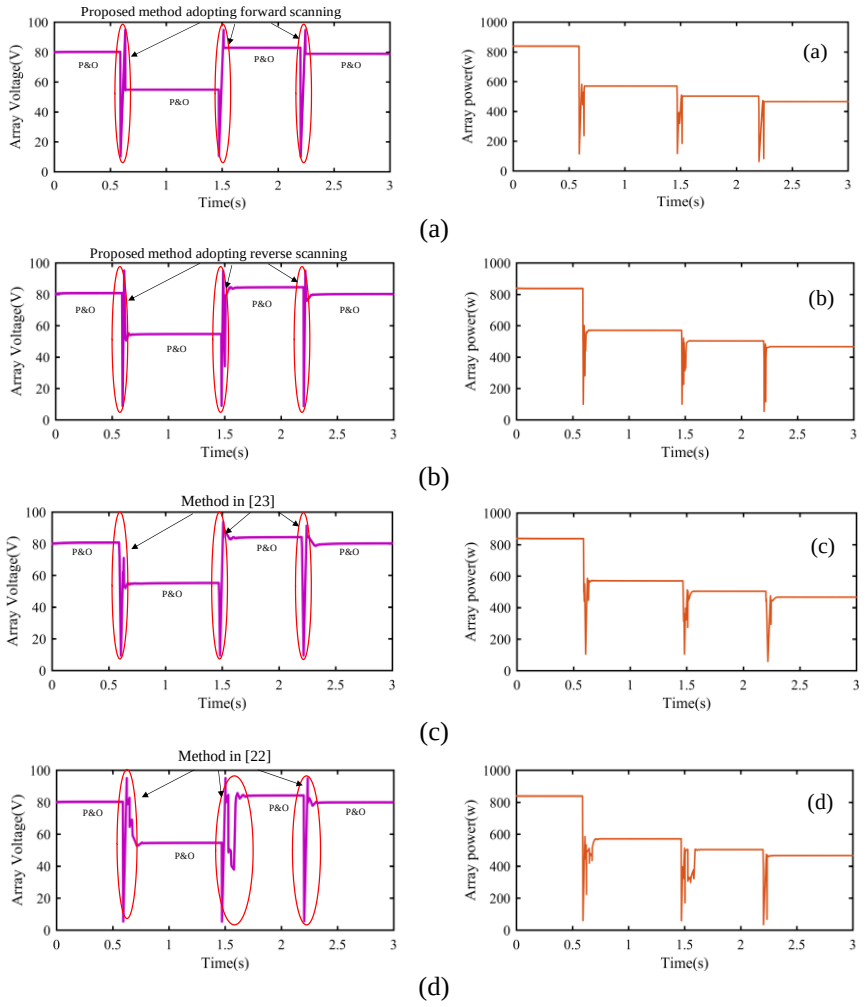

Figure 12. Comparison between the proposed and other algorithms (a) the proposed method adopting the forward scanning, (b) the proposed method adopting the reverse scanning, (c) approximate I-V based method, and (d) PV current variation-based method

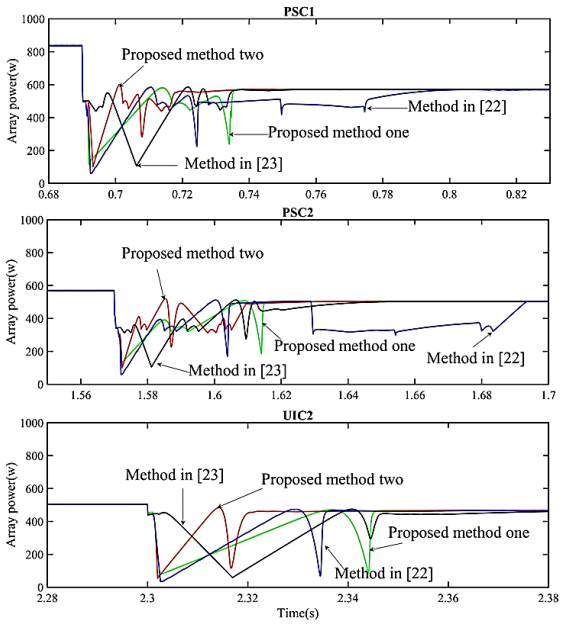

Figure 13. Zoom-in of the comparison between the proposed and other algorithms

Table 2. Comparison between the proposed and other algorithms developed for MPPT under PSCs

Method	Total Tracking time	Average power	Storing LMPPs	Calling the P&O
The proposed work integrating forward scanning	140 ms	571.64 watt	Yes	Once
The proposed work integrating reverse scanning	90 ms	573.33 watt	Yes	Once
The method in [23]	200 ms	570.84 watt	No	Once
The method in [22]	294 ms	567.77 watt	Yes	Number of LMPPs

5. EXPERIMENTAL VALIDATION

The LabVIEW CompactRIO 9063 is used to validate the proposed method experimentally, as shown in Figure 14. The current is sensed using shunt resistance and interfaced to NI9225 analog to digital converter. The PV voltage is interfaced directly to the NI9225. Three PV modules (PS M36s-100W) manufactured by Philadelphia Soler are connected in series. The used PV module has the data as listed in Table 3.

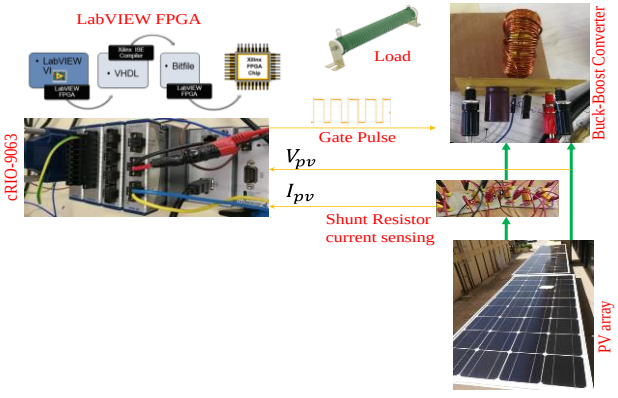

Figure 14. Experimental setup test-bed

Table 3. Data of PV module PS M36s-100W

Parameters	Value
P_{mpp}	100 ± 3% W
V_{oc}	22.64 V
I_{sc}	5.72 A
V_{mpp}	18.39 V
I_{mpp}	5.44 A

Four scenarios are considered to validate the proposed work; the data for each scenario has been collected and listed in Table 4. The first scenario has no partial shadow; in this case, the proposed algorithm detects only one peak at 50.17 V, and the P&O locates the exact GMPP at 47.86 V. One of the PV modules faces a partial shadow in the second scenario. The scanning stage of the proposed method locates two QLMPPs at 41.07 and 55.25 V, respectively. The maximum at 41.07 V is given to the tracking stage, and the P&O finds the exact GMPP at 39.09 V.

The third test is for two partially shaded modules. In this case, three peaks are detected; the maximum among them is given to the P&O to find the exact GMPP. Finally, all of the modules are facing different irradiances. In this case, three peaks are detected; the maximum among them is given to the P&O to find the exact GMPP. The results listed in Table 4 validate the applicability of the proposed MPPT algorithm in locating the GMPP under partial shading conditions.

Table 4. Experimental test data under different irradiances

Partial Shading condition			$LMPP_1$		$LMPP_2$		$LMPP_3$		GMPP	
PV_1	PV_2	PV_3	V_1	P_1	V_2	P_2	V_3	P_3	$V_{P\&O}$	$P_{P\&O}$
—	—	—	50.17	182.29	—	—	—	—	47.86	191.23
—	PS	—	41.07	150.51	55.25	115.37	—	—	39.09	156.7
PS	PS	—	30.69	119.69	44.89	108.67	55.23	114.12	30.25	121.08
PS	PS	PS	21.58	87.07	44.92	108.22	55.2	113.44	54.49	115.4

6. CONCLUSION

An algorithm to extract the maximum power from the PV-based generation systems under non-uniform weather, with the ability to detect and bypass the hidden point in the partially shaded P–V curve, is presented in this paper. PSHP is caused by a transition between GMPP to an LMPP once the partial shading patterns have been changed, which is hard to be observed monitoring the power difference alone. Three simple stages form the proposed algorithm: the scanning stage in which all the quasi-maximum power points are located and stored. The maximum of these points is passed to the second stage to find the exact GMPPT employing P&O. A hidden point stage is adopted to bypass the PSHP in the P–V curve if it exists. The reverse scanning procedure is integrated with the proposed work to minimize the search space. The performance indices of the proposed GMPPT algorithm, compared with other algorithms developed for MPPT under PSCs, are better in terms of the generated power and the time to track the actual global peak. The proposed MPPT algorithm is two times faster than the compared methods, generating almost 2% extra power. Besides the simulation verification, the proposed MPPT algorithm is implemented in real-time using NI Compact-RIO in FPGA mode to demonstrate the viability of the proposed work.

ACKNOWLEDGEMENTS

Besides the open-access fees, the deanship of research at Jordan University of Science and Technology supported the findings in this paper under grant number 20180250.

REFERENCES

[1] I. Smadi and R. AL-Qudah, "Explicit one-step model and adaptive maximum power point tracking algorithm for a photovoltaic module," *Computers & Electrical Engineering*, vol. 85, p. 106659, 2020, doi: 10.1016/j.compeleceng.2020.106659.

[2] A. AL-Ramaden and I. A. Smadi, "Partial Shading Detection and Global MPPT Algorithm for PV System," *2019 IEEE Jordan International Joint Conference on Electrical Engineering and Information Technology (JEEIT)*, 2019, pp. 135-140, doi: 10.1109/JEEIT.2019.8717442.

[3] H. Mirazizi and M. Shafiyi, "A comprehensive analysis of partial shading effect on output parameters of a grid-connected PV system," *International Journal of Electrical and Computer Engineering (IJECE)*, vol. 8, no. 2, pp. 749–762, 2018, doi: 10.11591/ijece.v8i2.pp749-762.

[4] M. H. Al-Jumaili, A. S. Abdalkafor, and M. Q. Taha, "Analysis of the hard and soft shading impact on photovoltaic module performance using solar module tester," *International Journal of Power Electronics and Drive System (IJPEDS)*, vol. 10, no. 2, pp. 1014–1021, Jun. 2019, doi: 10.11591/ijpeds.v10.i2.pp1014-1021.

[5] H. Attia and S. Ulusoy, "A new perturb and observe MPPT algorithm based on two steps variable voltage control," *International Journal of Power Electronics and Drive Systems (IJPEDS)*, vol. 12, no. 4, pp. 2201–2208, Dec. 2021, doi:10.11591/ijpeds.v12.i4.

[6] S. Kollimalla and M. Mishra, "A novel adaptive P&O MPPT algorithm considering sudden changes in the irradiance," *IEEE Transactions on Energy Conversion*, vol. 29, no. 3, pp. 602–610, 2014, doi: 10.1109/tec.2014.2320930.

[7] K. Saidi, M. Maamoun, and M. Bounekhla, "A new high performance variable step size perturb-and-observe MPPT algorithm for photovoltaic system," *International Journal of Power Electronics and Drive Systems (IJPEDS)*, vol. 10, no. 3, pp. 1662–1674, Sep. 2019, doi: 10.11591/ijpeds.v10.i3.pp1662-1674.

[8] F. Zhang, K. Thanapalan, A. Procter, S. Carr, and J. Maddy, "Adaptive hybrid maximum power point tracking method for a photovoltaic system," *IEEE Transactions on Energy Conversion*, vol. 28, no. 2, pp. 353–360, 2013, doi: 10.1109/tec.2013.2255292.

[9] M. Al-Dhaifallah, A. Nassef, H. Rezk, and K. Nisar, "Optimal parameter design of fractional order control based INC-MPPT for PV system," *Solar Energy*, vol. 159, pp. 650–664, Jan. 2018, doi: 10.1016/j.solener.2017.11.040.

[10] M. Moutchou and A. Jbari, "Fast photovoltaic IncCond-MPPT and backstepping control, using DC-DC boost converter," *International Journal of Electrical and Computer Engineering (IJECE)*, vol. 10, no. 1, pp. 1101–1112, Feb. 2020, doi: 10.11591/ijece.v10i1.pp1101-1112.
[11] M. Atig, Y. Miloud, A. Miloudi, and A. Merah, "A novel optimization of the particle swarm based maximum power point tracking for photovoltaic systems under partially shaded conditions," *International Journal of Power Electronics and Drive Systems (IJPEDS)*, vol. 12, no. 3, pp. 1795–1803, Sep. 2021, doi: 10.11591/ijpeds.v12.i3.pp1795-1803.
[12] X. Gao, F. Deng, H. Zheng, N. Ding, Z. Ye, Y. Cai, and X. Wang, "Followed the regularized leader (FTRL) prediction model based photovoltaic array reconfiguration for mitigation of mismatch losses in partial shading condition," *IET Renew. Power Gener.* vol. 16, no. 1, pp. 159–176, 2021, doi: 10.1049/rpg2.12275.
[13] M. Baka, P. Manganiello, D. Soudris, and F. Catthoor, "A cost-benefit analysis for reconfigurable PV modules under shading," *Solar Energy*, vol. 178, pp. 69–78, 2019, doi: 10.1016/j.solener.2018.11.063.
[14] D. Pilakkat and S. Kanthalakshmi, "An improved P&O algorithm integrated with artificial bee colony for photovoltaic systems under partial shading conditions," *Solar Energy*, vol. 178, pp. 37–47, Jan. 2019, doi: 10.1016/j.solener.2018.12.008.
[15] D. K. Mathi and R. Chinthamalla, "A hybrid global maximum power point tracking method based on butterfly particle swarm optimization and perturb and observe algorithms for a photovoltaic system under partially shaded conditions," *International Transactions on Electrical Energy Systems*, vol. 30, no. 10, p. e12543, Jul. 2020, doi: 10.1002/2050-7038.12543.
[16] M. A. Mohamed, A. A. Diab, and H. Rezk, "Partial shading mitigation of PV systems via different meta-heuristic techniques," *Renewable energy*, vol. 130, pp. 1159–1175, Jan. 2019, doi: 10.1016/j.renene.2018.08.077.
[17] H. Rezk, *et al.*, "A novel statistical performance evaluation of most modern optimization-based global MPPT techniques for partially shaded PV system," *Renewable and Sustainable Energy Reviews*, vol. 115, p. 109372, Nov. 2019, doi: 10.1016/j.rser.2019.109372.
[18] H. Patel and V. Agarwal, "Maximum power point tracking scheme for PV systems operating under partially shaded conditions," *IEEE transactions on industrial electronics*, vol. 55, no. 4, pp. 1689–1698, 2008, doi: 10.1109/TIE.2008.917118.
[19] M. Boztepe, F. Guinjoan, G. Velasco-Quesada, S. Silvestre, A. Chouder, and E. Karatepe, "Global MPPT scheme for photovoltaic string inverters based on restricted voltage window search algorithm," *IEEE Transactions on Industrial Electronics*, vol. 61, no. 7, pp. 3302–3312, 2014, doi: 10.1109/TIE.2013.2281163.
[20] Y. H. Liu, J. H. Chen, and J. W. Huang, "Global maximum power point tracking algorithm for PV systems operating under partially shaded conditions using the segmentation search method," *Solar Energy*, vol. 103, pp. 350–363, May 2014, doi: 10.1016/j.solener.2014.02.031.
[21] M. A. Ghasemi, H. M. Foroushani, and M. Parniani, "Partial shading detection and smooth maximum power point tracking of PV arrays under PSC," *IEEE Transactions on Power Electronics*, vol. 31, no. 9, pp. 6281–6292, 2015, doi: 10.1109/TPEL.2015.2504515.
[22] A. Ramyar, H. Iman-Eini, and S. Farhangi, "Global maximum power point tracking method for photovoltaic arrays under partial shading conditions," *IEEE Transactions on Industrial Electronics*, vol. 64, no. 4, pp. 2855–2864, 2016, doi: 10.1109/TIE.2016.2632679.
[23] M. A. Ghasemi, A. Ramyar, and H. Iman-Eini, "MPPT method for PV systems under partially shaded conditions by approximating I–V curve," *IEEE Transactions on industrial electronics*, vol. 65, no. 5, pp. 3966–3975, 2017, doi:10.1109/TIE.2017.2764840.
[24] K. L. Shenoy, C. G. Nayak, and R. P. Mandi, "Effect of partial shading in grid connected solar pv system with FL controller," *International Journal of Power Electronics and Drive Systems (IJPEDS)*, vol. 12, no. 1, pp. 431–440, Mar. 2021, doi: 10.11591/ijpeds.v12.i1.pp431-440.
[25] I. Yadav, S. K. Maurya, and G. K. Gupta, "A literature review on industrially accepted MPPT techniques for solar PV system," *International Journal of Electrical and Computer Engineering (IJECE)*, vol. 10, no. 2, pp. 2088–8708, Apr. 2020, doi: 10.11591/ijece.v10i2.pp2117-2127.

BIOGRAPHIES OF AUTHORS

Issam A. Smadi is an IEEE senior member. He is currently the acting chairman of the Electrical Engineering Department and an Associate Professor with the Jordan University of Science and Technology, Irbid, Jordan. His research interests include integrating renewable energy in power systems, control in power electronics, dynamic state estimation, electric drives, power system dynamics, and control. He can be contacted at email: iasmadi@just.edu.jo.

Ahmad AL-Ramaden was born in 1993. He received the B.Sc. and M.Sc degrees in electrical engineering, especially in power and control, from the Jordan University of Science and Technology, Irbid, Jordan, in 2016 and 2019, respectively. Currently, he is with Chart General Construction Company, Amman, Jordan, working as a site maintenance electrical engineer. His research interests include control, algorithms, and simulation of photovoltaic systems. He can be contacted at email: ahmadtr2@hotmail.com.